



Full Length Articles

Contributions of dynamic venous blood volume versus oxygenation level changes to BOLD fMRI

Xiaopeng Zong, Tae Kim*, Seong-Gi Kim

Neuroimaging Laboratory, Department of Radiology, University of Pittsburgh, Pittsburgh, PA 15203, USA

ARTICLE INFO

Article history:

Accepted 19 February 2012

Available online 28 February 2012

Keywords:

CBV
BOLD
BOLD undershoot
Cerebral arterial blood volume
Cerebral venous blood volume
Venous oxygenation level

ABSTRACT

Blood-oxygenation-level-dependent (BOLD) fMRI has contributions from venous oxygenation and venous cerebral blood volume (CBV) changes. To examine the relative contribution of venous CBV change (ΔCBV_v) to BOLD fMRI, BOLD and arterial CBV changes (ΔCBV_a) to a 40-s forepaw stimulation in six α -chloralose anesthetized rats were measured using a magnetization transfer-varied fMRI technique, while total CBV change (ΔCBV_t) was measured with injection of iron oxide nanoparticles. ΔCBV_v was obtained by subtracting ΔCBV_a from ΔCBV_t . We observed a fast ΔCBV_a response with a time constant of 2.9 ± 2.3 s and a slower ΔCBV_v response with a time constant of 13.5 ± 5.7 s and an onset delay of 6.1 ± 3.3 s. These results are consistent with earlier studies under different anesthesia and stimulus, supporting that fast CBV_a and slow CBV_v responses are generalizable. Assuming the observed post-stimulus BOLD undershoot is at least partly explained by the ΔCBV_v contribution, the relative contribution of the ΔCBV_v - and oxygenation-change-related components to the BOLD response was estimated. The relative ΔCBV_v contribution increases with time during stimulation; whereby it is <0.14 during initial 10 s and reaches a maximum possible value of ~ 0.45 relative to the oxygenation contribution during the 30–40 s period after stimulus onset. Our data indicates that the contribution of venous oxygenation change to BOLD fMRI is dominant for short stimulations.

© 2012 Elsevier Inc. All rights reserved.

Introduction

Blood-oxygenation-level-dependent (BOLD) functional magnetic resonance imaging (fMRI) is a widely used non-invasive tool for studying brain functions. Despite its name, BOLD fMRI signal is dependent not only on blood oxygenation level (Y), but also on venous cerebral blood volume (CBV_v) changes. While increased Y reduces the amount of paramagnetic de-oxyhemoglobin (dHb) in the blood, and thus increases field homogeneity, increased CBV_v increases the amount of dHb in a given imaging pixel. To the first order approximation, the BOLD signal change can be expressed as a sum of the oxygenation level change (ΔY) and the CBV_v change (ΔCBV_v)-related components ($\text{BOLD}_{\Delta Y}$ and $\text{BOLD}_{\Delta\text{CBV}_v}$, respectively) (Kim et al., 1999).

A quantitative understanding of the dynamic BOLD fMRI response requires a determination of the dynamics of its $\text{BOLD}_{\Delta Y}$ and $\text{BOLD}_{\Delta\text{CBV}_v}$ contributions. Earlier studies have estimated $\text{BOLD}_{\Delta Y}$ and $\text{BOLD}_{\Delta\text{CBV}_v}$ contributions in the steady state during prolonged stimulation (Kennan et al., 1998; Leite et al., 2002; Scheffler et al., 1999), assuming similar total cerebral blood volume (CBV_t) and CBV_v (Scheffler et al., 1999; Kennan et al., 1998; Leite et al., 2002). However, the dynamic evolutions of $\text{BOLD}_{\Delta Y}$ and $\text{BOLD}_{\Delta\text{CBV}_v}$ have not been characterized. In our previous compartment-specific CBV studies, the CBV_t changes during neural

stimulation occur mainly in arteries, rather than in veins, for a 15-s rat somatosensory stimulation (Kim et al., 2007). When relatively long stimulation duration (40-s) is applied in cat's visual cortex (Kim and Kim, 2011), initial rapid arterial dilation is followed by slower prolonged venous dilation. Thus, the measurement of dynamic CBV_v changes is needed to determine its contribution to BOLD fMRI signals.

The above-mentioned compartment-specific CBV studies were performed with isoflurane anesthesia (Kim et al., 2007; Kim and Kim, 2011). However, most of the functional CBV MRI studies in animal models have been accomplished under α -chloralose anesthesia (Silva et al., 1999; Mandeville et al., 1998; Lee et al., 2001; Silva et al., 2007; Hyder, 2004; Kerskens et al., 1996). It is known that different anesthesia agents induce different baseline conditions of vessel physiology, which results in different functional signal changes (Masamoto et al., 2007). In baseline (e.g., resting) condition, CBF in rats under isoflurane anesthesia (~ 130 – 200 ml/100 g/min) (Wegener and Wong, 2008; Kim and Kim, 2005; Kim et al., 2007; Sicard et al., 2003) is substantially higher than under α -chloralose anesthesia (~ 60 – 80 ml/100 g/min) (Tsekos et al., 1998; Lee et al., 2001; Kida et al., 2004). During somatosensory stimulation, CBF increased by $\sim 20\%$ under isoflurane anesthesia (Kim et al., 2007), while it increased by ~ 80 – 150% under α -chloralose anesthesia (Lee et al., 2002; Silva et al., 1999; Kida et al., 2004). Higher baseline CBF resulted in slower stimulus-induced BOLD and CBF responses (Ances et al., 2001; Cohen et al., 2002; Bakalova et al., 2001). Thus, it remains unclear whether the dynamic characteristics of ΔCBV_a and ΔCBV_v

* Corresponding author at: Department of Radiology, University of Pittsburgh, 3025 E Carson Street, Room 156, Pittsburgh, PA 15203, USA. Fax: +1 412 383 6799.

E-mail address: tak19@pitt.edu (T. Kim).

responses during neural activation under α -chloralose are the same as our previous findings under isoflurane anesthesia (Kim and Kim, 2011).

To characterize the dynamic $BOLD_{\Delta Y}$ versus $BOLD_{\Delta CBV_v}$ contributions to BOLD response and evaluate their anesthesia dependence, we measured total CBV (ΔCBV_t) and arterial CBV changes (ΔCBV_a) in α -chloralose anesthetized rats by contrast agent (Mandeville et al., 1998; Kennan et al., 1998) and a magnetization transfer (MT)-varied fMRI technique (Kim et al., 2008; Kim and Kim, 2010), respectively. Then, ΔCBV_v was obtained as the difference between ΔCBV_t and ΔCBV_a . Assuming the observed post-stimulus BOLD undershoot is at least partly explained by the ΔCBV_v contribution (0–100%), we determined the $BOLD_{\Delta CBV_v}$ and $BOLD_{\Delta Y}$ time courses. To investigate the anesthesia dependence of the relative $BOLD_{\Delta Y}$ and $BOLD_{\Delta CBV_v}$ contributions, the same analysis was also carried out for our earlier cat visual-stimulation data obtained under isoflurane anesthesia (Kim and Kim, 2011).

Theories

MT-varied fMRI for ΔCBV_a measurement

Details of the theoretical background and implementation of the MT-varied fMRI were reported previously (Kim et al., 2008; Kim and Kim, 2010). Briefly, in BOLD fMRI studies, neural stimulation-induced signal changes from arterial blood and tissue can be separated by their different magnetization transfer (MT) properties. The tissue signal is dependent on the MT effect induced by off-resonance RF pulses. In contrast, the arterial blood pool experiences only a minimal MT effect due to the inflow of fresh blood spins unaffected by the MT-inducing pulses. If capillary water freely exchanges with tissue water, this upstream exchange could generate MT effects in venous blood similar to those in the tissue. Even if capillary water does not freely exchange with the tissue, the venous blood contribution to MR signal could be ignored due to its short transverse relaxation time ($T_2 < 10$ ms) at 9.4 T (Lee et al., 1999). Therefore, extravascular tissue and intravascular venous blood pools can be considered together as one MT-dependent compartment. Thus, the signal in an imaging voxel originates from MT-dependent and MT-independent compartments. The power of the MT-inducing pulses was varied in different fMRI runs. When we linearly fit normalized stimulus-induced signal change with MT ($\Delta S_{MT}/S_0$) versus normalized baseline MR signal (S_{MT}/S_0), where S_0 is the signal at fully relaxed condition, the intercept (b) at $S_{MT}/S_0 = 0$ is related to ΔCBV_a by (Kim and Kim, 2010):

$$\Delta CBV_a = b \cdot \lambda \cdot e^{(R_{2,artery}^* - R_{2,tissue}^*) \cdot TE}, \quad (1)$$

where $\lambda = 0.9$ ml/g is the tissue-to-blood water partition coefficient (Herscovitch and Raichle, 1985). In cases of $|R_{2,artery}^* - R_{2,tissue}^*| \ll 1/TE$, the exponential term is close to one. Under our experimental condition of $TE = 20$ ms, this condition is not satisfied well. Therefore, $R_{2,tissue}^*$ and $R_{2,artery}^*$ were measured for accurate quantification of ΔCBV_a .

The ΔCBV_a value measured by MRI represents the blood volume within arterial vessels of all sizes, and includes a portion of capillaries carrying blood water before exchange with tissue water, while ΔCBV_v is the remainder of ΔCBV_t excluding ΔCBV_a .

BOLD responses induced by ΔY and ΔCBV_v

When the fractional deoxy-hemoglobin level ($\Delta Y/(1 - Y_0)$) and fractional CBV_v changes ($\Delta CBV_v/CBV_{v0}$) are much less than 1, the BOLD response can be separated into ΔCBV_v and ΔY -related components:

$$BOLD = BOLD_{\Delta Y} + BOLD_{\Delta CBV_v} = TE\alpha^* \left[\frac{\Delta Y}{1 - Y_0} - \frac{\Delta CBV_v}{\beta \cdot CBV_{v0}} \right], \quad (2)$$

where Y_0 and CBV_{v0} are baseline venous blood oxygenation level and baseline CBV_v , respectively, β is an exponent relating deoxy-hemoglobin level and R_2^* : $R_2^* \propto (1 - Y)^\beta$, and α^* is a region and animal-specific constant (Kim et al., 1999). Alternative BOLD signal models (Obata et al., 2004; Davis et al., 1998) have been proposed, which can all be reduced to Eq. (2) under the conditions of $\Delta Y/(1 - Y_0) \ll 1$ and $\Delta CBV_v/CBV_{v0} \ll 1$.

Methods and materials

Animal preparation and stimulation

Eleven male Sprague–Dawley rats weighing 300–450 g (Charles River Laboratories, Wilmington, MA, USA) were studied; six for the BOLD, ΔCBV_a , and ΔCBV_t measurements under α -chloralose anesthesia and five for the determination of arterial blood and tissue R_2^* values under isoflurane. The animal protocol was approved by the University of Pittsburgh Animal Care and Use Committee. The animals were initially anesthetized with 5% isoflurane in a mixture of O_2 and air gases (total O_2 concentration of ~30% throughout the experiments). The animals were intubated and the isoflurane level was subsequently reduced to 2% during the surgical procedure. The femoral artery and vein were catheterized for blood pressure/heart rate monitoring, and for fluid administration and injection of contrast agent, respectively. The rats were then transferred to a custom MRI-compatible cradle equipped with a water-circulating heating pad. The heads of the animals were carefully secured in a stereotaxic restrainer before placement in the magnet.

For BOLD, ΔCBV_a , and ΔCBV_t measurements, 30 mg/kg bolus of α -chloralose was injected and isoflurane was gradually reduced to 0% within the first hour after bolus injection. Then continuous α -chloralose infusion started after the first hour at 30 mg/kg/h, mixed with 0.05 ml/kg/h of dextrose and 1.2 mg/kg/h of pancuronium bromide throughout the experiments. For R_2^* measurements, animal anesthesia was maintained with 1.4% isoflurane without α -chloralose because, in contrast to α -chloralose anesthesia, isoflurane dilates blood vessels in the brain (Farber et al., 1997) and thus enhances blood MR signal. Rectal temperature was continuously maintained at 37.5 ± 0.5 °C with a feedback controlled heating pad (Digi-Sense Temperature Controller R/S, Cole-Parmer, IL, USA). The end-tidal CO_2 was maintained at 3.5–4.5% and arterial blood gas was periodically measured.

For forepaw stimulation, two needle electrodes were inserted under the skin between digits 2 and 3, and between digits 3 and 4 of the left forepaw (Silva et al., 1999). Stimulation was applied to the animal through a constant-current stimulator (A365D, World Precision Instruments Inc., Sarasota, FL, USA) that was gated by a pulse generator (Master 8, AMPI, Israel) with the following optimized parameters (Silva et al., 1999): current = 1.5–2 mA depending on the rat by ensuring no blood pressure change during the stimulation, pulse duration = 333 μ s, and repetition rate = 3 Hz. The stimulation duration was 40 s and the inter-stimulation intervals were ~2 min.

MRI methods

All MRI experiments were performed on a 9.4 T/31 cm magnet with an actively shielded 12-cm gradient coil, which is interfaced to a Unity INOVA console (Varian, Palo Alto, CA, USA). A 2-cm diameter surface coil was used for all functional studies, while two actively detunable RF coils were used for baseline arterial T_2^* measurement: a neck coil for ASL (arterial spin labeling) and a head coil for imaging. The homogeneity of the magnetic field was optimized by localized shimming. Preliminary multi-slice scout BOLD fMRI studies were performed to localize the primary somatosensory cortex (S1), then a single 2-mm thick coronal slice showing robust BOLD response in S1 was selected for further studies. All images were acquired with the GE-EPI

sequence. Two separate studies were performed: 1) R_2^* of arterial blood was measured at baseline (no activation) and 2) functional studies were performed to measure BOLD, arterial CBV, and total CBV changes.

Baseline measurements of cortical arterial blood and tissue R_2^*

R_2^* of tissue and cortical arterial blood was measured for ΔCBV_a quantification (see Eq. (1)). Since the arterial blood transit time from labeling plane to capillary is 600–700 ms in rats (Kim and Kim, 2006), we chose arterial spin labeling duration of 700 ms without a post-labeling delay. Thus, labeled spins mostly fill the arterial vasculature during the 700 ms of labeling period and do not exchange with tissue due to the ~500-ms water exchange time between capillary and tissue (Orrison et al., 1995). Labeled and control images were alternately acquired using the single-shot GE EPI with matrix size = 64×32 , field of view (FOV) = $3.0 \times 1.5 \text{ cm}^2$, repetition time (TR) = 2.5 s, and echo time (TE) = 6, 10, 15, and 20 ms. TE-dependent signal intensity was obtained from two 3×3 -pixel ($1.4 \times 1.4 \text{ mm}^2$) regions of interest (ROI) centered over the S1 of both hemispheres. Then, R_2^* values of tissue and cortical arterial blood were determined from the slopes of linear fits of $\log(\text{unlabeled control signal})$ and $\log(\text{difference between labeled and control signals})$ vs. TE, respectively.

Measurements of ΔCBV_a and $\Delta CBV_t/CBV_0$

BOLD and ΔCBV_a measurements with MT-varied fMRI were followed by $\Delta CBV_t/CBV_0$ studies without MT effects after injection of a susceptibility contrast agent, where CBV_0 is the baseline CBV_t . All images were acquired with TR = 1 s, TE = 20 ms for MT-varied BOLD and TE = 10.5 ms for $\Delta CBV_t/CBV_0$ studies, flip angle ~50° in S1, in-plane matrix = 64×64 , and FOV = $2.3 \times 2.0 \text{ cm}^2$. Each fMRI run consisted of consecutive 20-s pre-stimulation, 40-s forepaw stimulation, and 80-s (for BOLD and ΔCBV_a) or 120-s (for CBV_t) post-stimulation periods, and repeated approximately 20 times for signal averaging.

MT-varied fMRI (Kim et al., 2008; Kim and Kim, 2010) was acquired using single-shot GE-EPI with the following MT-inducing pulse parameters: offset frequency = 5000 Hz, pulse duration = 880 ms, and MT ratios ($MTR = (1 - S_{MT}/S)$, where S_{MT} and S are the intensities with and without MT pulses, respectively) = 0, ~0.5, and ~0.75 in the S1 region.

For the determination of stimulus-induced CBV_t change ($\Delta CBV_t/CBV_0$), the FDA-approved susceptibility contrast agent Feraheme (AMAG Pharmaceuticals, Inc., MA) was injected intravenously with a concentration of ~10 mg Fe/kg body weight. The steady-state condition was achieved within 5 min after the injection. In order to reduce TE, a two-shot EPI technique was used. For the calculation of Feraheme-induced R_2^* changes (ΔR_2^*), gradient-echo EPI images were acquired with 11 different TE values between 11 and 50 ms before and after Feraheme injection.

Functional MRI data processing

General analysis

Data analyses were performed by custom MATLAB (Mathworks, Natick, MA, USA) routines. For each animal, all runs with identical experimental conditions were averaged. The mean time courses were then corrected for possible baseline linear drifts by fitting a linear function to the last 15-s of the pre-stimulation and the last 20-s of the post-stimulation periods, and subtracting the resulting fit from the original time courses (Bandettini et al., 1993).

BOLD fMRI signals were obtained from the fMRI data with MTR = 0 (no MT effect), and ΔCBV_a was determined from the fMRI data with MTR values of 0, ~0.5, and ~0.75. For normalization of the MT-varied fMRI time courses for ΔCBV_a calculation, S_0 was determined by extrapolating to the first time point ($t=0$) by fitting the 2nd–7th time points of the MR signal intensity time courses with MTR = 0 with the theoretical steady-state-approaching curve,

because the first image was acquired for EPI reference scan with zero phase encoding. Then, normalized functional signal changes ($\Delta S_{MT}/S_0$) were linearly fitted against normalized mean baseline signals (S_{MT}/S_0), and ΔCBV_a (units of ml blood/g tissue) was calculated from the intercept using Eq. (1).

The $\Delta CBV_t/CBV_0$ ratio was calculated from the Feraheme-induced baseline R_2^* change and the fMRI data without MT effect. Baseline R_2^* values were calculated by fitting a single-exponential function of TE-dependent image intensity versus TE, then the baseline R_2^* change induced by Feraheme injection ($\Delta R_{2,\text{contrast}}^*$) was determined from the difference of R_2^* values before and after injection. Stimulation-induced R_2^* changes before and after Feraheme injection (denoted as $\Delta R_{2,\text{stim}}^*$ and $\Delta R_{2,\text{stim,contrast}}^*$, respectively) were calculated as $-\ln(\Delta S/S)/TE$, where ΔS is the stimulation-induced MRI signal change at MTR = 0. The fractional total CBV change ($\Delta CBV_t/CBV_0$) was then calculated as:

$$\frac{\Delta CBV_t}{CBV_0} = \frac{\Delta R_{2,\text{stim,contrast}}^* - \Delta R_{2,\text{stim}}^*}{\Delta R_{2,\text{contrast}}^*}, \quad (3)$$

where $\Delta R_{2,\text{stim}}^*$ was subtracted from $\Delta R_{2,\text{stim,contrast}}^*$ to correct for the BOLD contribution to the stimulation-induced R_2^* change.

Generation of BOLD, ΔCBV_a , and $\Delta CBV_t/CBV_0$ maps

Functional maps were generated with AFNI (Cox, 1996). All images were smoothed with a 2D Gaussian filter ($\sigma = 0.15 \text{ mm}$). Functional signal changes at the three MT levels, ΔCBV_a and $\Delta CBV_t/CBV_0$ amplitudes were calculated as their mean responses of the 5–40th time points after stimulus onset. All color maps were displayed for pixels with $P < 0.001$ in the fMRI responses at all three MTR levels and in the total CBV-weighted response.

Quantitative ROI analysis of BOLD, ΔCBV_a , and ΔCBV_t

Since a rat brain atlas (Paxinos and Watson, 1986) shows a forelimb S1 of $\sim 1.5 \times 1.5 \text{ mm}^2$ in coronal plates 0.2 and 0.3 mm anterior to bregma, a 4×5 pixel ($1.4 \times 1.6 \text{ mm}^2$) ROI centered over anatomically-defined area on the hemisphere contra-lateral to the stimulated forepaw was defined for all CBV_a and CBV_t quantifications. Time courses were obtained from the ROI in each animal from raw data, and ΔCBV_a and $\Delta CBV_t/CBV_0$ time courses were calculated as described above. To reduce noise levels, time courses were smoothed with a 3-point ordered statistical filter (Cox, 1996) by replacing the n th data point by $0.15 \times \min(d_{n-1}, d_n, d_{n+1}) + 0.7 \times \text{median}(d_{n-1}, d_n, d_{n+1}) + 0.15 \times \max(d_{n-1}, d_n, d_{n+1})$, where d_n is the value of n th data point in the original time courses and the functions min, median, and max return the minimum, median, and maximum values of their arguments, respectively.

To compare ΔCBV_a and ΔCBV_t , baseline CBV_t value (CBV_0) was assumed within a physiological range; an upper bound was 5 ml/100 g, while a lower bound was estimated by matching the time courses of the initial ΔCBV_t (= fractional CBV_t change $\times CBV_0$) and ΔCBV_a responses, assuming that the initial ΔCBV_t response mainly originates from the dilation of arteries (Kim et al., 2007; Vazquez et al., 2010; Drew et al., 2011). Since the ΔCBV_a response reached a peak at 5–6 s after stimulus onset, CBV_0 was calculated from the ratio of the mean ΔCBV_a and mean fractional CBV_t changes of the 5–6 second data points after stimulus onset. Then, ΔCBV_v values were calculated as the difference of the ΔCBV_t and ΔCBV_a time courses (Kim and Kim, 2011).

In order to characterize the dynamics of functional CBV changes, the time course of each blood volume component was fitted by a 40-s boxcar with unit height convoluted with the following single-exponential impulse response function (IRF):

$$f(t) = \frac{a}{\tau} \exp\left(-\frac{t-t_0}{\tau}\right) h(t-t_0), \quad (4)$$

where $h(t-t_0) = 1$ for $t \geq t_0$ and is 0 otherwise. The parameter a is equal to the steady-state response to a very long stimulation, and τ is the time constant. The response delay t_0 is either assumed to be zero or treated as a free parameter in the fit (see Results for details).

Determination of ΔCBV_v -induced BOLD response ($\text{BOLD}_{\Delta\text{CBV}_v}$)

To estimate $\text{BOLD}_{\Delta\text{CBV}_v}$, the post-stimulus BOLD undershoot was assumed to be originated at least partially from the sustained ΔCBV_v . Thus, $\text{BOLD}_{\Delta\text{CBV}_v} = c \times \Delta\text{CBV}_v = f_{\text{CBV}_v} \times \text{BOLD}$ undershoot, where c is a factor relating ΔCBV_v to $\text{BOLD}_{\Delta\text{CBV}_v}$, and f_{CBV_v} is the fraction of $\text{BOLD}_{\Delta\text{CBV}_v}$ in the BOLD signal during the post-stimulus BOLD undershoot, ranging between 0 and 1. When $f_{\text{CBV}_v} = 1$, the post-stimulus BOLD undershoot is caused entirely by ΔCBV_v . The value of c can be calculated as the product of f_{CBV_v} and the ratio of BOLD to ΔCBV_v responses during the post-stimulus undershoot. Then $\text{BOLD}_{\Delta\text{CBV}_v}$ was calculated over the whole time course as $(c \times \Delta\text{CBV}_v$ time course), and the difference between the experimental BOLD data and $\text{BOLD}_{\Delta\text{CBV}_v}$ is the BOLD signal induced by oxygenation level changes ($\text{BOLD}_{\Delta Y}$).

The same analysis was also carried out for our previous published BOLD and ΔCBV_v time courses in cats under isoflurane anesthesia (Kim and Kim, 2011). In that study, the stimulation consisted of 40-s binocular, full-field, black-and-white square-wave moving gratings, which was presented between 50-s pre-stimulation and 100-s post-stimulation periods of static gratings. For both studies, the factor c was calculated using the mean BOLD and ΔCBV_v responses near the dip of the post-stimulus BOLD undershoot (from the dip to the time point with $\sim 3/4$ the dip value). Bar plots of the ratios of the mean $\text{BOLD}_{\Delta\text{CBV}_v}$ to $\text{BOLD}_{\Delta Y}$ were presented for periods of 0–10 s, 10–20 s, 20–30 s, 30–40 s, and 10–40 s after stimulation onset assuming $f_{\text{CBV}_v} = 1/3, 2/3, \text{ or } 1.0$.

Results

All animals were maintained within a normal physiological range ($\text{PaCO}_2 = 31.6 \pm 4.5$ (mean \pm SEM) mm Hg; $\text{PaO}_2 = 131.1 \pm 9.5$ mm Hg, $\text{pH} = 7.48 \pm 0.01$). No significant arterial blood pressure change

was observed during stimulation. The measured R_2^* of tissue and cortical arterial blood was $35.8 \pm 4.3 \text{ s}^{-1}$ (mean \pm SEM, $n = 5$) and $50.7 \pm 5.3 \text{ s}^{-1}$, respectively, in the somatosensory cortical area. This gives $e^{-(R_{2, \text{artery}}^* - R_{2, \text{tissue}}^*) \cdot \text{TE}} = 0.74 \pm 0.10$ at $\text{TE} = 20 \text{ ms}$, which was incorporated for all ΔCBV_a calculations.

BOLD vs. arterial CBV vs. venous CBV change induced by stimulation

Fig. 1 shows fractional fMRI signal change maps of one animal (Fig. 1A), and the group-averaged fMRI time courses ($n = 6$) of the S1 ROI (Fig. 1B) at the three MTR levels. As expected, baseline image intensities decreased with MTR (Fig. 1A), but percent signal change increased with MTR (Fig. 1B), which agrees well with the previous results (Kim et al., 2008; Kim and Kim, 2011; Kim and Kim, 2010). During the post-stimulus period (see inset time courses), prominent undershoots of the signal intensities below the pre-stimulus baseline were observed with similar amplitude at the three MTR levels in all animals.

Fig. 2A shows the ΔCBV_a and $\Delta\text{CBV}_t/\text{CBV}_0$ maps in a representative animal, where activation is clearly observed in right S1. Fig. 2B displays the group-averaged ΔCBV_a and $\Delta\text{CBV}_t/\text{CBV}_0$ time courses. CBV_a increased rapidly immediately following stimulus onset and was maintained at a plateau during the remainder of the 40-s stimulation period, while CBV_t had an initial rapid increase followed by a slow increase during the remainder of the stimulation period. After stimulus offset, CBV_a quickly returned to pre-stimulus baseline and was followed by a slight undershoot, while CBV_t slowly decreased to baseline. The dynamics of $\Delta\text{CBV}_t/\text{CBV}_0$ time course agrees well with previous findings in rats under similar α -chloralose anesthetic conditions (Mandeville et al., 1998; Silva et al., 2007).

In order to obtain absolute ΔCBV_t , two different conditions were assumed: i) mean $\Delta\text{CBV}_a = \text{mean } \Delta\text{CBV}_t$ at the peak (5–6 s after stimulus onset), and ii) $\text{CBV}_0 = 5 \text{ ml}/100 \text{ g}$. When we assumed that mean $\Delta\text{CBV}_a = \text{mean } \Delta\text{CBV}_t$ at the peak, we obtained a CBV_0 value of $3.9 \text{ ml}/100 \text{ g}$, which is within the range ($1.6\text{--}4.1 \text{ ml}/100 \text{ g}$) of CBV_0 for the rat's gray matter previously reported in the literature (Tropres et al., 2001; Kim et al., 2007; Schwarzbauer et al., 1997; Lin et al., 1997;

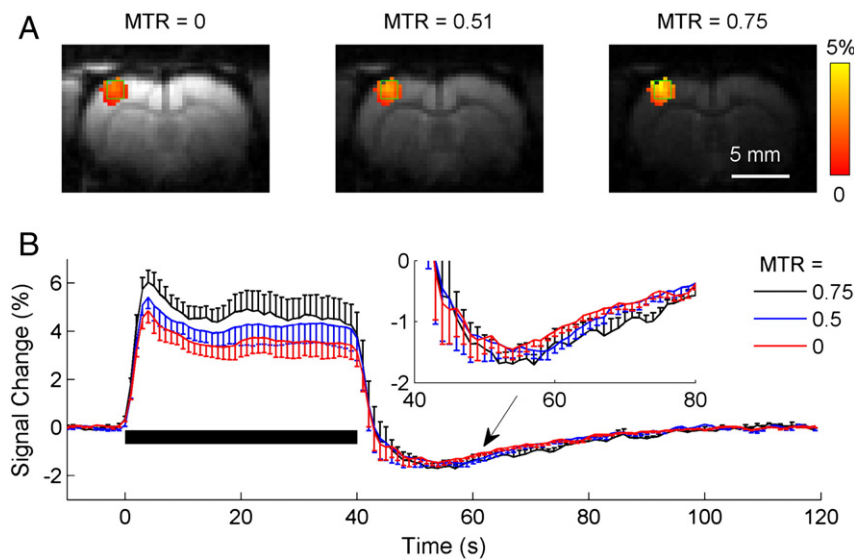


Fig. 1. BOLD response amplitude maps (A) and group-averaged time courses (B) in the magnetization transfer (MT)-BOLD fMRI experiment for arterial cerebral blood volume changes (ΔCBV_a). (A) The green box denotes the region of interest (ROI) in the primary somatosensory cortex. The magnetization transfer ratios (MTR) are given above each image. The response amplitudes are calculated as the mean of the 5th–40th time points after stimulus onset. (B) The black horizontal bar denotes the time period when the stimulus was on. The inset figure is a magnification of the post-stimulus undershoot period. Error bars: standard errors of the group mean. (For interpretation of the references to color in this figure legend, the reader is referred to the web version of this article.)

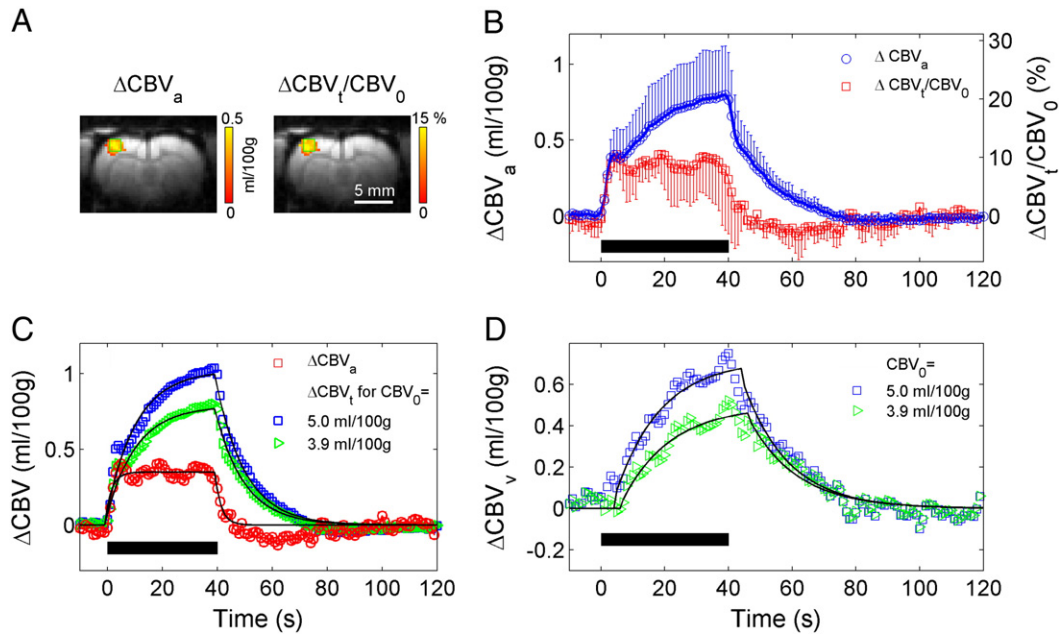


Fig. 2. Maps of ΔCBV_a and relative total CBV response (ΔCBV_a and $\Delta\text{CBV}_t/\text{CBV}_0$) amplitudes (A) and group averaged ΔCBV_a and $\Delta\text{CBV}_t/\text{CBV}_0$ (B), ΔCBV_a and ΔCBV_t (C), and ΔCBV_v (D) response time courses. (A) The green box denotes the region of interest (ROI) in the somatosensory cortex. (C) ΔCBV_t was estimated by assuming two possible values of baseline CBV (CBV_0) (3.9 and 5 ml/100 g tissue). Black lines are fits using a single exponential impulse response (Eq. (4) with $t_0 = 0$) convoluted with a boxcar function. (D) Corresponding ΔCBV_v responses were obtained by subtracting ΔCBV_a from ΔCBV_t . Black lines are fits using a single exponential impulse response (Eq. (4) with t_0 as a free parameter) convoluted with a boxcar. The black horizontal bars in (B)–(D) denote the stimulation period. Best fits are given in Table 1. Error bars: standard deviations. (For interpretation of the references to color in this figure legend, the reader is referred to the web version of this article.)

Adam et al., 2003). ΔCBV_t time courses were determined as $(\Delta\text{CBV}_t/\text{CBV}_0) \times \text{CBV}_0$ (Fig. 2C). The ΔCBV_v response (subtraction of ΔCBV_a from ΔCBV_t) is much slower than the ΔCBV_a response for both assumed CBV_0 values (Fig. 2D), which is consistent with our previous findings in isoflurane-anesthetized cats (Kim and Kim, 2011). Fig. 3 displays the percentage of mean ΔCBV_v in ΔCBV_t for periods 0–10 s, 10–20 s, 20–30 s, 30–40 s, and 10–40 s after stimulus onset. The ΔCBV_v is not significant during the initial 10 s and increases to 56–66% during the last 10 s of the stimulation period.

Least-square fits to the group-averaged ΔCBV_a , ΔCBV_t , and ΔCBV_v responses were performed by convolution of a unit boxcar with the IRF of Eq. (4) (solid lines in Figs. 2C and D). The response delay (t_0 in Eq. (4)) was set to zero for fits to ΔCBV_a and ΔCBV_t (Fig. 2C) due to their fast initial increase following stimulation. Since the ΔCBV_v response seemed to deviate from zero after several seconds from

stimulus onset, it was fitted by treating t_0 as a free parameter (black lines in Fig. 2D). To compare with results in Kim and Kim (2011), we also fitted the ΔCBV_v response by setting $t_0 = 0$. Table 1 lists the steady-state amplitudes (a), single exponential time constants (τ), and delays (t_0) of the fitted ΔCBV_t , ΔCBV_v , and ΔCBV_a responses for the two assumed CBV_0 values. From the fitted values of a for ΔCBV_a and ΔCBV_v , we can conclude that the ΔCBV_v response contributes 58–67% of the total CBV response in the steady-state, very close to its contribution during the last 10 s of stimulation.

To study inter-animal variations, fits were also carried out in individual animals assuming $\Delta\text{CBV}_a = \Delta\text{CBV}_t$ at 5–6 s from stimulus. Reliable fits could be obtained in most cases except for the ΔCBV_a response in one rat and for the ΔCBV_v response when $t_0 \neq 0$ in another rat. The fitted τ for ΔCBV_a was in the range of 1.1–6.9 s (2.9 ± 2.3 s (mean \pm SD), $n = 5$). The fitted τ for ΔCBV_v was in the range of 15.6–27.8 s (21.9 ± 4.6 s, $n = 6$) for fixed $t_0 = 0$ and in the range of 6.7–21.8 s (13.5 ± 5.7 s, $n = 5$) for free t_0 with fitted t_0 of 2.3–9.5 s (6.1 ± 3.3 s, $n = 5$). The mean values of τ and t_0 did not differ significantly from their values obtained from fitting the group-averaged time courses with $\text{CBV}_0 = 3.9$ ml/100 g ($p > 0.58$; t -test). The fitted steady-state mean amplitude of the ΔCBV_a was 0.42 ± 0.13 ml/100 g,

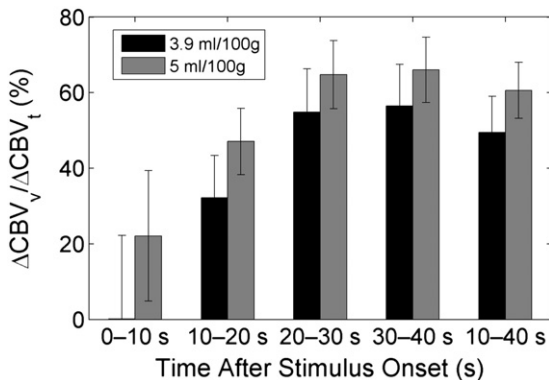


Fig. 3. The percentage of ΔCBV_v in ΔCBV_t during different periods of the stimulation. Two total baseline CBV_0 values of 3.9 and 5 ml/100 g are assumed. The error bars are standard errors of the mean.

Table 1

Characteristics of functional CBV_a , CBV_t and CBV_v responses. Delays t_0 , time constants (τ) and amplitudes (a) in Eq. (4) were obtained by fitting the group-averaged time courses (Figs. 2C and D) using Eq. (4) convoluted with a unit boxcar stimulus function. Two baseline CBV_0 conditions were used. The units of the baseline CBV_t and a are ml-blood/100 g tissue.

Baseline CBV_t	ΔCBV_t		ΔCBV_v (no delay)		ΔCBV_v (with delay)		ΔCBV_a		
	τ (s)	a	τ (s)	a	τ (s)	t_0 (s)	a	τ (s)	a
3.9	10.7	0.80	23.2	0.54	15.0	6.5	0.49	2.4	0.35
5.0	10.7	1.02	18.9	0.77	14.2	4.1	0.72		

consistent with the steady-state amplitudes of the group-averaged ΔCBV_a time course ($p=0.28$). The fitted steady-state mean amplitude of the ΔCBV_t response was 0.90 ± 0.21 ml/100 g, also consistent with the steady-state amplitude of the group-averaged ΔCBV_t time course with $\text{CBV}_0 = 3.9$ ml/100 g ($p=0.31$). The fitted steady-state amplitude of the ΔCBV_v response was 0.65 ± 0.17 ml/100 g when $t_0 = 0$ and was 0.63 ± 0.11 ml/100 g when $t_0 \neq 0$, which were consistent with the corresponding fitted values of the group-averaged ΔCBV_v time course with $\text{CBV}_0 = 3.9$ ml/100 g ($p > 0.05$).

Contributions of venous oxygenation level versus venous CBV change to BOLD

The BOLD response shows a prominent post-stimulus undershoot which returns to baseline at a time point similar to the ΔCBV_v response, suggesting that the slow return of ΔCBV_v is at least partly responsible for the BOLD undershoot, i.e. $f_{\text{CBV}_v} > 0$. Figs. 4A and B display $\text{BOLD}_{\Delta Y}$ and $\text{BOLD}_{\Delta\text{CBV}_v}$ time courses for the f_{CBV_v} range of 0–1 for this rat study and our earlier cat data (Kim and Kim, 2011), respectively. In Figs. 4A and B, CBV_0 values were set to match initial ΔCBV_a and ΔCBV_t responses; $\text{CBV}_0 = 3.9$ ml/100 g in Fig. 4A and $\text{CBV}_0 = 5.08$ ml/100 g in Fig. 4B after correction of the tissue–arterial blood R_2^* difference (Kim and Kim, 2011). The upper and lower boundary of the red region is $\text{BOLD}_{\Delta Y}$ at $f_{\text{CBV}_v} = 1$ and 0, respectively, while the upper and lower boundary of the green region is $\text{BOLD}_{\Delta\text{CBV}_v}$ at $f_{\text{CBV}_v} = 0$ and 1, respectively. Figs. 4C and D show ratios of mean $\text{BOLD}_{\Delta\text{CBV}_v}$ to mean $\text{BOLD}_{\Delta Y}$ for the rat and cat studies, respectively, for periods of 0–10 s, 10–20 s, 20–30 s, 30–40 s, and 10–40 s after stimulation onset for $f_{\text{CBV}_v} = 0.33$, 0.67, and 1. In Fig. 4C, the ratios for $\text{CBV}_0 = 3.9$ ml/100 g and 5 ml/100 g correspond to gray bars and superimposed white bars, respectively, while the ratios were calculated for $\text{CBV}_0 = 5.08$ ml/100 g only in Fig. 4D. In both studies, $|\text{BOLD}_{\Delta\text{CBV}_v}|$ was less than 15% of $\text{BOLD}_{\Delta Y}$ during the first 10-s period and increased with time during the later periods of stimulation. When $f_{\text{CBV}_v} = 1$, its absolute value reaches

~45% of $\text{BOLD}_{\Delta Y}$ during the last 10-s period of stimulation, which corresponds to a 45% reduction of the BOLD response compared to the case of no ΔCBV_v change. Furthermore, when $f_{\text{CBV}_v} = 1$, the ratio of mean $\text{BOLD}_{\Delta\text{CBV}_v}$ to mean $\text{BOLD}_{\Delta Y}$ over the 10–40 s period is -0.34 ± 0.07 ($\text{CBV}_0 = 3.9$ ml/100 g) to -0.40 ± 0.06 ($\text{CBV}_0 = 5$ ml/100 g) for rat data and -0.34 ± 0.09 for cat data.

Discussions

R_2^* of arterial blood and tissue

In our study, we found that the cortical arterial blood R_2^* (50.7 ± 5.3 s $^{-1}$) is higher than the tissue R_2^* (35.8 ± 4.3 s $^{-1}$). The tissue R_2^* agrees well with a recently reported R_2^* of 35.3 s $^{-1}$ in the gray matter of human brain (Budde et al., 2011) at the same field strength of 9.4 T. Tissue T_2 in the rat somatosensory cortex at 9.4 T is 37.7 ± 0.7 ms (Meng et al., 2011) to 38.6 ± 2.1 ms (Lee et al., 1999), while cortical arterial blood T_2 is 30.6 ± 4.0 ms in vivo (Meng et al., 2011), consistent with a higher cortical arterial blood R_2^* compared to tissue. However, femoral arterial blood T_2 measured in vitro is 40.8 ± 3.4 ms (Lee et al., 1999). The shorter cortical arterial blood T_2 compared to the in-vitro femoral arterial T_2 might be explained by the motion of arterial blood during measurements and slightly reduced oxygenation in cortical arteries (e.g., 82–88%) compared to the systemic level (e.g., 97%) (Vazquez et al., 2010).

In contrast to a larger R_2^* of the cortical arterial blood compared to the tissue at 9.4 T, the opposite is true at low fields. At 1.5 T, R_2^* is in the range of 4–7 s $^{-1}$ for fully oxygenated in vitro arterial blood (Spees et al., 2001; Li et al., 1998). For blood samples with Y and hematocrit levels similar to our study (Y=0.82 and Hct~0.4), the R_2^* is approximately equal to 7 s $^{-1}$ (Spees et al., 2001), while some other studies found R_2^* ranging from 9 to 10.5 s $^{-1}$ (Li et al., 1998; Silvennoinen et al., 2003; Chien et al., 1994). On the other hand, R_2^* in gray matter of human brain is about 15 s $^{-1}$ at 1.5 T (Gati et al.,

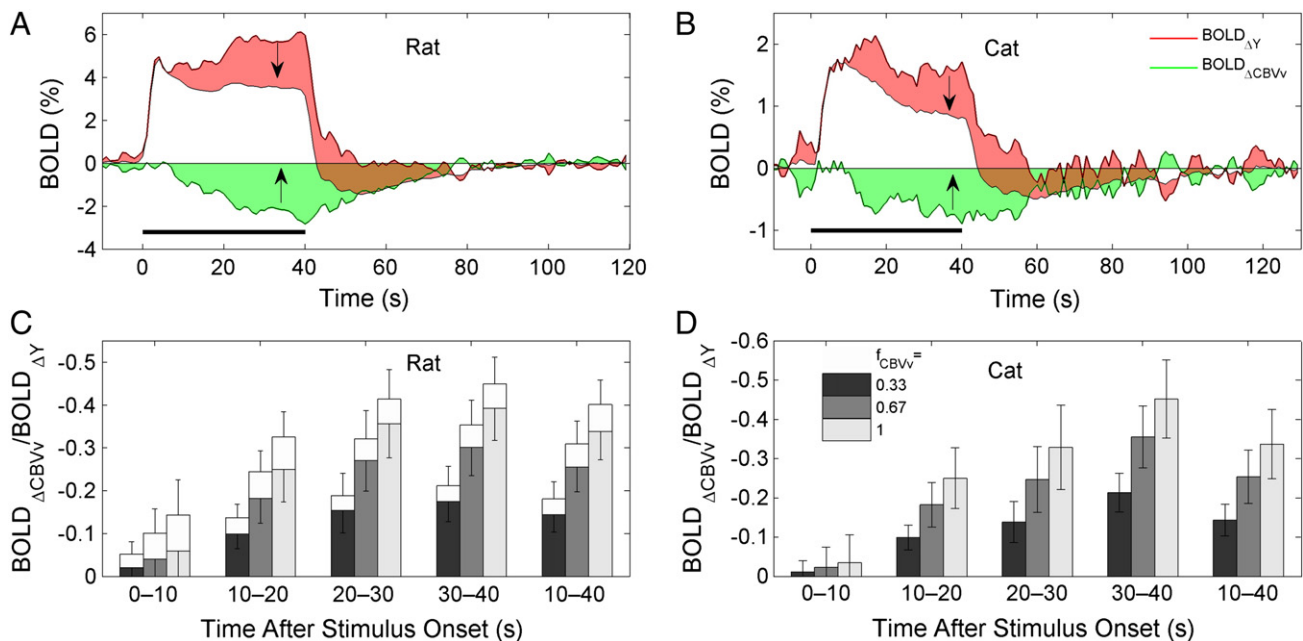


Fig. 4. Decomposition of BOLD responses into venous CBV ($\text{BOLD}_{\Delta\text{CBV}_v}$) and venous blood oxygenation level ($\text{BOLD}_{\Delta Y}$) change related components in the current rat (A and C) and earlier cat studies (B and D). (A) and (B): The top boundary of red region and the bottom boundary of the green region are $\text{BOLD}_{\Delta Y}$ and $\text{BOLD}_{\Delta\text{CBV}_v}$ time courses, respectively, when BOLD undershoot is solely caused by $\text{BOLD}_{\Delta\text{CBV}_v}$, i.e. $f_{\text{CBV}_v} = 1$. The arrows denote the directions the two time courses would move with decreasing f_{CBV_v} . The lower boundary of the red region and the upper boundary of the green region corresponds to $f_{\text{CBV}_v} = 0$. Black horizontal bars: stimulation period. (C) and (D): The ratio of $\text{BOLD}_{\Delta\text{CBV}_v}$ to $\text{BOLD}_{\Delta Y}$ during different periods of the stimulation for assumed f_{CBV_v} values of 0.33, 0.67, and 1. In (C), the gray and superimposed white bars correspond to $\text{CBV}_0 = 3.9$ and 5 ml/100 g, respectively. In (D), CBV_0 is set to 5.08 ml/100 g. (For interpretation of the references to color in this figure legend, the reader is referred to the web version of this article.)

1997; Peters et al., 2007). The different relative R_2^* values of the arterial blood and tissue at 1.5 T and 9.4 T might be explained by a linear (Peters et al., 2007) and superlinear (Thulborn et al., 1982) field dependence of the tissue and blood R_2^* values, respectively.

By assuming equal values of $R_{2,artery}^*$ and $R_{2,tissue}^*$ in our previous work, the ΔCBV_a values are believed to be underestimated by $26 \pm 10\%$ (Kim and Kim, 2011; Kim and Kim, 2010), in which a GE-EPI sequence with TE = 20 ms was used. Accordingly, the ΔCBV_t and ΔCBV_v responses were also underestimated in our original papers, but correct values were used here. The correction of different R_2^* values does not change the relative contributions of arterial versus venous responses and the dynamic behaviors of the compartment-specific CBV responses.

Comparison to earlier results under the same anesthetic condition

In this study, we found an initial fast CBV_a response with a time constant of 2.9 ± 2.3 s and a subsequent slower CBV_v response with a time constant of 13.5 ± 5.7 s in α -chloralose anesthetized rats. The CBV_v response was delayed 6.1 ± 3.3 s from the stimulation onset. Our results are consistent with earlier studies under the same anesthesia conditions (Silva et al., 2007; Mandeville et al., 1999; Lu et al., 2005), where both fast and slow components were observed in the total CBV or CBV-weighted responses. In (Mandeville et al., 1999), the fast and slow CBV-weighted response components have time constants of 1.5 ± 0.8 s and 14 ± 13 s, respectively, and the onset of the slow component is delayed by 8 s relative to the stimulus onset. In (Silva et al., 2007), the total CBV impulse response was modeled as a sum of two gamma variate functions, where the fast function had a time to peak (TTP) of 1.29 s and a full width at half maximum (FWHM) of 1.18 s, and the slow function had a TTP of 7.3 s and a FWHM of 18.2 s. To convert those values to slow response delays and time constants defined in Eq. (4), we note that the TTP corresponds roughly to the response delay in our impulse response function and the FWHM is roughly related to the single exponential time constant by $\tau = \text{FWHM}/(2 \ln 2)$, which is obtained by setting the FWHM of the gamma variate function equal to the FWHM of a symmetric single exponential function $f(t) = \exp(-|t|/\tau)$. Therefore, the time constants of the fast and slow components in Silva et al. (2007) are 0.85 and 13.1 s, respectively, and the delay of the slow component is 7.3 s.

The relative contributions of the fast and slow components in our study are also in good agreement with the earlier studies. In Mandeville et al. (1999) and Silva et al. (2007), the slow component of the CBV response contributes approximately 40% and 67%, respectively, of the total CBV response by the end of 30-s stimulation, close to our result where ΔCBV_v was $55 \pm 12\%$ of ΔCBV_t at 20–30 s after stimulus onset when $CBV_0 = 3.9$ ml/100 g (see Fig. 3). In Lu et al. (2005), fast and slow components were clearly visible in their total CBV-weighted response to 32-s whisker stimulation in the barrel cortex. The slow component contributed roughly 50% of the total CBV change by the end of the 32-s stimulation.

One interesting note is that the prediction of the total CBV response to long stimulation based on its response to short stimulation

will underestimate the actual response due to ignoring slow ΔCBV_v , which was indeed observed in Lu et al. (2005).

Anesthesia dependence of hemodynamic responses

Table 2 summarizes the time constants of the slow and fast CBV responses studied in different anesthesia conditions and species. Although different anesthetics induce different baseline vascular and physiological conditions, fast and slow CBV responses were consistently observed. A human fMRI study with direct ΔCBV_v measurement also found a slower ΔCBV_v response than CBF change (CBF change is highly correlated with ΔCBV_a ; Kim et al., 2007) (Chen and Pike, 2009).

The peak amplitudes of the ΔCBV_a and ΔCBV_v in α -chloralose anesthetized rats are higher than those in isoflurane anesthetized cats: 0.35 ml/100 g versus 0.24 ml/100 g for ΔCBV_a and 0.46–0.68 ml/100 g versus 0.18 ml/100 g (at $CBV_0 = 5.08$ ml/100 g) for ΔCBV_v (Kim and Kim, 2011). Note that the values for cats have been corrected for the tissue-cortical arterial blood R_2^* difference.

Relative contributions of $BOLD_{\Delta CBV_v}$ and $BOLD_{\Delta Y}$ to BOLD

We examined $BOLD_{\Delta CBV_v}$ and $BOLD_{\Delta Y}$ contributions to BOLD for the whole possible f_{CBV_v} range of 0–1. When $f_{CBV_v} = 0$, CBV_v change does not contribute to the BOLD response, while when $f_{CBV_v} = 1$, $|BOLD_{\Delta CBV_v}|$ reaches its maximum possible value and the BOLD post-stimulus undershoot is caused solely by the slow return of ΔCBV_v . During the initial 10-s stimulation period, the CBV_v change has negligible contribution to the BOLD response in both cat and rat studies for all f_{CBV_v} values, suggesting that the dynamic BOLD response to short (<10 s) stimulation mainly reflects dynamic venous blood oxygenation changes. However, the $BOLD_{\Delta CBV_v}$ becomes more significant with time for longer stimulations. During the 30–40-s period, the BOLD response can be maximally reduced by 45% due to the negative $BOLD_{\Delta CBV_v}$ contribution. The $|BOLD_{\Delta CBV_v}|$ can be as large as 40% of $BOLD_{\Delta Y}$ over the period of 10–40 s after stimulus onset (Fig. 3). This upper limit is similar to reductions of 35 to 46% in BOLD during prolonged stimulation by ΔCBV_v as reported in earlier studies (Kennan et al., 1998; Scheffler et al., 1999; Leite et al., 2002). However, we note that the values estimated in Kennan et al. (1998) and in Scheffler et al. (1999) might be overestimated because of the assumption of similar CBV_t and CBV_v in their calculations.

The increase of $|BOLD_{\Delta CBV_v}|$ with time during stimulation might be responsible for 1) the reduced BOLD response after initial overshoot as observed in the current and some other fMRI studies (Obata et al., 2004; Kim and Kim, 2011; Hoge et al., 1999; Frahm et al., 1996), and 2) the nonlinearity of BOLD fMRI responses. 1) Based on Balloon model simulations (Buxton et al., 1998), Obata et al. (2004) demonstrated that, due to increased ΔCBV_v with time, the BOLD response decreases after initial overshoot even when the assumed CBF response continuously increases with time during stimulation. Thus, the effect of dynamic ΔCBV_v changes needs to be considered in interpreting the dynamic properties of BOLD responses to long stimulations. 2) The predicted BOLD response to long stimulation based on

Table 2
Comparison of the single exponential time constants of the fast and slow CBV impulse response components in different studies. The fast and slow components correspond to the arterial and venous CBV responses, respectively, in our study. SMA – somatosensory cortex.

Study	Species	Cortical area	Anesthesia	τ (fast or ΔCBV_a) (s)	τ (slow or ΔCBV_v) (s)	Delay of slow component (s)	Measurements
Mandeville et al. (1999)	Rat	SMA	α -chloralose	1.5 ± 0.8	14 ± 13	8	ΔCBV_t
Leite et al. (2002)	Monkey	Visual	Awake	4.5	13.5	1.5	ΔCBV_t
Silva et al. (2007)	Rat	SMA	α -chloralose	0.85	13.1	7.3	ΔCBV_t
Kim and Kim (2011)	Cat	Visual	Isoflurane	2.5	18.4–40.9	Fixed to 0	$\Delta CBV_t, \Delta CBV_a$
Drew et al. (2011)	Mouse	Primary vibrissa	Awake	10 ± 10	40 ± 35	Fixed to 0	Vessel size
This study	Rat	SMA	α -chloralose	2.4	14.2–15.0	4.1–6.5	$\Delta CBV_t, \Delta CBV_a$

the BOLD IRF with minimal ΔCBV_v contribution to short stimulation would be higher than the experimental BOLD with the ΔCBV_v contribution. This explanation was consistent with the findings of Miller et al. (2001), although other sources of nonlinearity should also be considered such as neural adaptation and nonlinearity in CBF responses.

Conclusions

In summary, we measured dynamic BOLD and compartment-specific CBV responses to electrical forepaw stimulation in α -chloralose anesthetized rats. The measured ΔCBV_a and ΔCBV_v time courses in rats under α -chloralose anesthesia show a fast ΔCBV_a response and a much slower and delayed ΔCBV_v response. Our findings support the anesthesia independence of the fast CBV_a and slow CBV_v dynamic properties. The obtained ΔCBV_v and BOLD time courses allowed us to estimate a range of the ΔCBV_v and oxygenation change related components in the BOLD response. The $|\text{BOLD}_{\Delta\text{CBV}_v}|$ is negligible during the initial 10 s of stimulation but may become significant toward the end of the stimulation period.

Acknowledgments

We thank Dr. Alex Poplawsky for helpful suggestions and Dr. Ping Wang for animal preparations and animal surgery instructions. This work was supported by NIH grants EB003324, EB003375, and NS44589.

References

- Adam, J.-F., Elleaume, H., le Duc, G., Corde, S., Charvet, A.-M., Tropres, I., le Bas, J.-F., Esteve, F., 2003. Absolute cerebral blood volume and blood flow measurements based on synchrotron radiation quantitative computed tomography. *J. Cereb. Blood Flow Metab.* 23, 499–512.
- Ances, B.M., Greenberg, J.H., Detre, J.A., 2001. The effects of graded hypercapnia on the activation flow coupling response due to forepaw stimulation in alpha-chloralose anesthetized rats. *Brain Res.* 911, 82–88.
- Bakalova, R., Matsuura, T., Kanno, I., 2001. Frequency dependence of local cerebral blood flow induced by somatosensory hind paw stimulation in rat under normo- and hypercapnia. *Jpn. J. Physiol.* 51, 201–208.
- Bandettini, P.A., Jesmanowicz, A., Wong, E.C., Hyde, J.S., 1993. Processing strategies for time-course data sets in functional MRI of the human brain. *Magn. Reson. Med.* 30, 161–173.
- Budde, J., Shajan, G., Hoffmann, J., Ugurbil, K., Pohmann, R., 2011. Human imaging at 9.4 T using T_2^* -, phase-, and susceptibility-weighted contrast. *Magn. Reson. Med.* 65, 544–550.
- Buxton, R.B., Wong, E.C., Frank, L.R., 1998. Dynamics of blood flow and oxygenation changes during brain activation: the balloon model. *Magn. Reson. Med.* 39, 855–864.
- Chen, J.J., Pike, G.B., 2009. Origins of the BOLD post-stimulus undershoot. *Neuroimage* 46, 559–568.
- Chien, D., Levin, D.L., Anderson, C.M., 1994. MR gradient echo imaging of intravascular blood oxygenation: T_2^* determination in the presence of flow. *Magn. Reson. Med.* 32, 540–545.
- Cohen, E.R., Ugurbil, K., Kim, S.G., 2002. Effect of basal conditions on the magnitude and dynamics of the blood oxygenation level-dependent fMRI response. *J. Cereb. Blood Flow Metab.* 22, 1042–1053.
- Cox, R.W., 1996. AFNI: software for analysis and visualization of functional magnetic resonance neuroimages. *Comput. Biomed. Res.* 29, 162–173.
- Davis, T.L., Kwong, K.K., Weisskoff, R.M., Rosen, B.R., 1998. Calibrated functional MRI: mapping the dynamics of oxidative metabolism. *Proc. Natl. Acad. Sci. U. S. A.* 95, 1834–1839.
- Drew, P.J., Shih, A.Y., Kleinfeld, D., 2011. Fluctuating and sensory-induced vasodynamics in rodent cortex extend arteriole capacity. *Proc. Natl. Acad. Sci. U. S. A.* 108, 8473–8478.
- Farber, N.E., Harkin, C.P., Niedfeldt, J., Hudetz, A.G., Kampine, J.P., Schmeling, W.T., 1997. Region-specific and agent-specific dilation of intracerebral microvessels by volatile anesthetics in rat brain slices. *Anesthesiology* 87, 1191–1198.
- Frahm, J., Kruger, G., Merboldt, K.D., Kleinschmidt, A., 1996. Dynamic uncoupling and recoupling of perfusion and oxidative metabolism during focal brain activation in man. *Magn. Reson. Med.* 35, 143–148.
- Gati, J.S., Menon, R.S., Ugurbil, K., Rutt, B.K., 1997. Experimental determination of the BOLD field strength dependence in vessels and tissue. *Magn. Reson. Med.* 38, 296–302.
- Herscovitch, P., Raichle, M.E., 1985. What is the correct value for the brain–blood partition coefficient for water? *J. Cereb. Blood Flow Metab.* 5, 65–69.
- Hoge, R.D., Atkinson, J., Gill, B., Crelier, G.R., Marrett, S., Pike, G.B., 1999. Stimulus-dependent BOLD and perfusion dynamics in human V1. *Neuroimage* 9, 573–585.
- Hyder, F., 2004. Neuroimaging with calibrated fMRI. *Stroke* 35, 2635–2641.
- Kennan, R.P., Scanley, B.E., Innis, R.B., Gore, J.C., 1998. Physiological basis for BOLD MR signal changes due to neuronal stimulation: separation of blood volume and magnetic susceptibility effects. *Magn. Reson. Med.* 40, 840–846.
- Kerskens, C.M., Hoehn-Berlage, M., Schmitz, B., Busch, E., Bock, C., Gyngell, M.L., Hossmann, K.A., 1996. Ultrafast perfusion-weighted MRI of functional brain activation in rats during forepaw stimulation: comparison with T2-weighted MRI. *NMR Biomed.* 9, 20–23.
- Kida, I., Maciejewski, P.K., Hyder, F., 2004. Dynamic imaging of perfusion and oxygenation by functional magnetic resonance imaging. *J. Cereb. Blood Flow Metab.* 24, 1369–1381.
- Kim, S.G., Rostrup, E., Larsson, H.B., Ogawa, S., Paulson, O.B., 1999. Determination of relative CMRO2 from CBF and BOLD changes: significant increase of oxygen consumption rate during visual stimulation. *Magn. Reson. Med.* 41, 1152–1161.
- Kim, T., Hendrich, K., Kim, S.G., 2008. Functional MRI with magnetization transfer effects: determination of BOLD and arterial blood volume changes. *Magn. Reson. Med.* 60, 1518–1523.
- Kim, T., Hendrich, K.S., Masamoto, K., Kim, S.G., 2007. Arterial versus total blood volume changes during neural activity-induced cerebral blood flow change: implication for BOLD fMRI. *J. Cereb. Blood Flow Metab.* 27, 1235–1247.
- Kim, T., Kim, S.-G., 2011. Temporal dynamics and spatial specificity of arterial and venous blood volume changes during visual stimulation: implication for BOLD quantification. *J. Cereb. Blood Flow Metab.* 31, 1211–1222.
- Kim, T., Kim, S.G., 2005. Quantification of cerebral arterial blood volume and cerebral blood flow using MRI with modulation of tissue and vessel (MOTIVE) signals. *Magn. Reson. Med.* 54, 333–342.
- Kim, T., Kim, S.G., 2006. Quantification of cerebral arterial blood volume using arterial spin labeling with intravoxel incoherent motion-sensitive gradients. *Magn. Reson. Med.* 55, 1047–1057.
- Kim, T., Kim, S.G., 2010. Cortical layer-dependent arterial blood volume changes: improved spatial specificity relative to BOLD fMRI. *Neuroimage* 49, 1340–1349.
- Lee, S.P., Duong, T.Q., Yang, G., Iadecola, C., Kim, S.G., 2001. Relative changes of cerebral arterial and venous blood volumes during increased cerebral blood flow: implications for BOLD fMRI. *Magn. Reson. Med.* 45, 791–800.
- Lee, S.P., Silva, A.C., Kim, S.G., 2002. Comparison of diffusion-weighted high-resolution CBF and spin-echo BOLD fMRI at 9.4 T. *Magn. Reson. Med.* 47, 736–741.
- Lee, S.P., Silva, A.C., Ugurbil, K., Kim, S.G., 1999. Diffusion-weighted spin-echo fMRI at 9.4 T: microvascular/tissue contribution to BOLD signal changes. *Magn. Reson. Med.* 42, 919–928.
- Leite, F.P., Tsao, D., Vanduffel, W., Fize, D., Sasaki, Y., Wald, L.L., Dale, A.M., Kwong, K.K., Orban, G.A., Rosen, B.R., Tootell, R.B., Mandeville, J.B., 2002. Repeated fMRI using iron oxide contrast agent in awake, behaving macaques at 3 Tesla. *Neuroimage* 16, 283–294.
- Li, D., Wang, Y., Waight, D.J., 1998. Blood oxygen saturation assessment in vivo using T_2^* estimation. *Magn. Reson. Med.* 39, 685–690.
- Lin, W., Paczynski, R.P., Kuppasamy, K., Hsu, C.Y., Haacke, E.M., 1997. Quantitative measurements of regional cerebral blood volume using MRI in rats: effects of arterial carbon dioxide tension and mannitol. *Magn. Reson. Med.* 38, 420–428.
- Lu, H., Soltysik, D.A., Ward, B.D., Hyde, J.S., 2005. Temporal evolution of the CBV-fMRI signal to rat whisker stimulation of variable duration and intensity: a linearity analysis. *Neuroimage* 26, 432–440.
- Mandeville, J.B., Marota, J.J., Kosofsky, B.E., Keltner, J.R., Weissleder, R., Rosen, B.R., Weisskoff, R.M., 1998. Dynamic functional imaging of relative cerebral blood volume during rat forepaw stimulation. *Magn. Reson. Med.* 39, 615–624.
- Mandeville, J.B., Marota, J.J.A., Ayata, C., Zaharchuk, G., Moskowitz, M.A., Rosen, B., Weisskoff, R., 1999. Evidence of a cerebrovascular postarteriole windkessel with delayed compliance. *J. Cereb. Blood Flow Metab.* 19, 679–689.
- Masamoto, K., Kim, T., Fukuda, M., Wang, P., Kim, S.G., 2007. Relationship between neural, vascular, and BOLD signals in isoflurane-anesthetized rat somatosensory cortex. *Cereb. Cortex* 17, 942–950.
- Meng, Y., Vazquez, A., Kim, S.-G., 2011. In vivo arterial blood T_2 measurement with arterial spin labeling at 9.4 Tesla. *Proc. Intl. Soc. Mag. Reson. Med.* 19, 372.
- Miller, K.L., Luh, W.M., Liu, T.T., Martinez, A., Obata, T., Wong, E.C., Frank, L.R., Buxton, R.B., 2001. Nonlinear temporal dynamics of the cerebral blood flow response. *Hum. Brain Mapp.* 13, 1–12.
- Obata, T., Liu, T.T., Miller, K.L., Luh, W.M., Wong, E.C., Frank, L.R., Buxton, R.B., 2004. Discrepancies between BOLD and flow dynamics in primary and supplementary motor areas: application of the balloon model to the interpretation of BOLD transients. *Neuroimage* 21, 144–153.
- Orrison, W., Lewine, J., Ja, S., Hartshorne, M.F., 1995. Functional Magnetic Resonance Imaging. Functional Brain Imaging. Mosby, St. Louis.
- Paxinos, G., Watson, C., 1986. The Rat Brain in Stereotaxic Coordinates. Academic Press, San Diego.
- Peters, A.M., Brookes, M.J., Hoogenraad, F.G., Gowland, P.A., Francis, S.T., Morris, P.G., Bowtell, R., 2007. T_2 measurements in human brain at 1.5, 3 and 7 T. *Magn. Reson. Imaging* 25, 748–753.
- Scheffler, K., Seifritz, E., Haselhorst, R., Bilecen, D., 1999. Titration of the BOLD effect: separation and quantitation of blood volume and oxygenation changes in the human cerebral cortex during neuronal activation and ferumoxide infusion. *Magn. Reson. Med.* 42, 829–836.
- Schwarzbauer, C., Morrissey, S.P., Deichmann, R., Hillenbrand, C., Syha, J., Adolf, H., Nöth, U., Haase, A., 1997. Quantitative magnetic resonance imaging of capillary water permeability and regional blood volume with an intravascular MR contrast agent. *Magn. Reson. Med.* 37, 769–777.
- Sicard, K., Shen, Q., Brevard, M.E., Sullivan, R., Ferris, C.F., King, J.A., Duong, T.Q., 2003. Regional cerebral blood flow and BOLD responses in conscious and anesthetized rats under basal and hypercapnic conditions: implications for functional MRI studies. *J. Cereb. Blood Flow Metab.* 23, 472–481.
- Silva, A.C., Koretsky, A.P., Duyn, J.H., 2007. Functional MRI impulse response for BOLD and CBV contrast in rat somatosensory cortex. *Magn. Reson. Med.* 57, 1110–1118.

- Silva, A.C., Lee, S.P., Yang, G., Iadecola, C., Kim, S.G., 1999. Simultaneous blood oxygenation level-dependent and cerebral blood flow functional magnetic resonance imaging during forepaw stimulation in the rat. *J. Cereb. Blood Flow Metab.* 19, 871–879.
- Silvennoinen, M.J., Clingman, C.S., Golay, X., Kauppinen, R.A., Van Zijl, P.C., 2003. Comparison of the dependence of blood R_2 and R_2^* on oxygen saturation at 1.5 and 4.7 Tesla. *Magn. Reson. Med.* 49, 47–60.
- Spees, W.M., Yablonskiy, D.A., Oswood, M.C., Ackerman, J.J., 2001. Water proton MR properties of human blood at 1.5 Tesla: magnetic susceptibility, $T(1)$, $T(2)$, $T^*(2)$, and non-Lorentzian signal behavior. *Magn. Reson. Med.* 45, 533–542.
- Thulborn, K.R., Waterton, J.C., Matthews, P.M., Radda, G.K., 1982. Oxygenation dependence of the transverse relaxation time of water protons in whole blood at high field. *Biochim. Biophys. Acta* 714, 265–270.
- Tropes, I., Grimault, S., Vaeth, A., Grillon, E., Julien, C., Payen, J.F., Lamalle, L., Decors, M., 2001. Vessel size imaging. *Magn. Reson. Med.* 45, 397–408.
- Tsekos, N.V., Zhang, F., Merkle, H., Nagayama, M., Iadecola, C., Kim, S.G., 1998. Quantitative measurements of cerebral blood flow in rats using the FAIR technique: correlation with previous iodoantipyrine autoradiographic studies. *Magn. Reson. Med.* 39, 564–573.
- Vazquez, A.L., Fukuda, M., Tasker, M.L., Masamoto, K., Kim, S.G., 2010. Changes in cerebral arterial, tissue and venous oxygenation with evoked neural stimulation: implications for hemoglobin-based functional neuroimaging. *J. Cereb. Blood Flow Metab.* 30, 428–439.
- Wegener, S., Wong, E.C., 2008. Longitudinal MRI studies in the isoflurane-anesthetized rat: long-term effects of a short hypoxic episode on regulation of cerebral blood flow as assessed by pulsed arterial spin labelling. *NMR Biomed.* 21, 696–703.